The neutral-to-ionic phase transition of TTF-CA: a Raman and infrared study versus temperature at atmospheric pressure

1996 J. Phys.: Condens. Matter 8 3553

(http://iopscience.iop.org/0953-8984/8/20/004)

J. Phys.: Condens. Matter **8** (1996) 3553–3567. Printed in the UK

The neutral-to-ionic phase transition of TTF-CA: a Raman and infrared study versus temperature at atmospheric pressure

A Moreac, A Girard, Y Delugeard and Y Marqueton

Groupe Matière Condensée et Matériaux, URA au CNRS 804 Université de Rennes I, Campus de Beaulieu, Bâtiment 11B, 35 042 Rennes Cédex, France

Received 2 January 1996

Abstract. The very first low-frequency infrared absorption and Raman scattering spectra of TTF-CA are presented. Several studies have been performed as a function of temperature at atmospheric pressure. In the neutral phase by infrared absorption, we have emphasized the critical behaviour of an antisymmetric lattice mode (located around 30 cm^{-1} at 150 K) which shows the displacive nature of the neutral-to-ionic phase transition of TTF-CA at atmospheric pressure. In the ionic phase, the Raman scattering study has permitted confirmation of this result, the soft mode being located around 105 cm^{-1} at 16 K. Besides, the Raman study of several totally symmetric internal modes has confirmed the clearly first-order character of this transition. Finally, this study permits an estimation of the e–mv (electron-molecular vibrations) coupling constants in the neutral and ionic phases.

1. Introduction

Organic π molecular donors (D) and acceptors (A) often form charge-transfer (CT) complexes in the solid state. These CT solids can be classified into two families: segregated ones where D and A molecules form segregated stacks, or mixed ones where D and A molecules alternate along the stacking axis.

For this second family, we can meet two kinds of CT complex according to the degree of charge transfer ρ: quasi-neutral complexes composed of nominally neutral molecules, or quasi-ionic complexes composed primarily of cations and anions. Under high pressure, several quasi-neutral complexes have been found [1] to undergo a phase transition into an ionic ground state. Much more rarely, at atmospheric pressure, this neutral-to-ionic phase transition can be induced [2, 3] at low temperature.

Moreover, the charge transfer energy $h\nu_{CT}$ which corresponds [4–6] to an intermolecular excitation of an electron from D to A, has a weak value ($h\nu_{CT} \approx 1$ eV) in these segregated and mixed CT complexes [1]. So, the interactions between vibrational modes and this CT excitation may have a relevant influence on the physical properties of these organic CT crystals and, more particularly, in the process of the neutral-to-ionic phase transition [7, 8]. This electron–phonon coupling is present in two forms [7, 8]: the electron–molecular vibrational coupling (e–mv) which involves the intramolecular modes, and the electron–lattice phonon coupling (e–lph) where electrons interact with the intermolecular modes.

In the case of mixed stacks, it has been shown that infrared spectra in the neutral phase and infrared and Raman spectra in the ionic phase are affected by the e–lph interactions,

0953-8984/96/203553+15$19.50

whereas Raman spectra in the neutral phase and Raman and infrared spectra in the ionic phase are affected by the e–mv coupling [7, 8].

The more typical example of a mixed CT complex showing a neutral-to-ionic phase transition is the tetrathialfulvalene-*p*-chloranile (TTF–CA) crystal (figure 1). Under high pressure [1, 9], ($P_{N-I} \approx 11$ kbar), this compound undergoes a neutral-to-ionic phase transition which can also be induced at low temperature [2, 3] ($T_{N-I} \approx 81$ K), presumably driven by the thermal contraction of the lattice.

It has been shown that this phase transition involves not only the ionicity ρ [2, 10] of the molecules, but also the one-dimensional stack structure [2, 3, 10, 11]. Indeed, a structural change corresponding to a dimerization, i.e. a formation of TTF–CA pairs along the stacking axis *a*, has been observed [12]. The space group of the high-temperature phase [12, 13] is $P2_1/n$ with two TTF–CA entities per unit cell and that of the low-temperature phase [12] is P_n also with two TTF–CA entities per unit cell. Furthermore, at the transition, the symmetry breaking [12] (loss of the helicoidal axis and of the centre of symmetry) shows that the structural instability is located at the Brillouin zone centre and that the symmetry of the order parameter is B_u. Therefore, infrared absorption and Raman scattering may be suitable techniques for the study of the critical dynamics in the neutral and ionic phases. Nevertheless, the clearly first-order character of this transition [2, 11] is an intrinsic difficulty for the observation of pretransitional phenomena. So far, no study has enabled the unambiguous definition of the nature of the transition mechanism. Only RQN [14] and electrical conductivity measurements [15] seem to show pretransitional dynamical phenomena. We also notice that calorimetric studies [16] point to a high entropy variation through the transition. This variation is near the $k \ln 2$ value which is generally characteristic of an order–disorder phase transition. However, by crystallographic analysis [12], no thermal agitation which might prove to be a characteristic of disorder has been observed in the neutral phase. So, infrared and Raman studies of the lattice dynamics might give useful information about the nature of the TTF–CA phase transition. Note that several infrared studies [9, 11, 17] have been performed on this transition, but the authors do not describe the evolution of the lattice dynamics and only the charge transfer evolution is studied [11]. In the same way, by Raman scattering, several authors [11, 18–20] have only investigated the e–mv coupling in the neutral and ionic phases. Thus, presently at atmospheric pressure, only a high temperature spectrum at 300 K and a low-temperature one at 15 K are known [11].

The present paper describes an infrared and Raman investigation of the neutral-to-ionic phase transition of TTF-CA. In section 2, the experimental conditions are given. Section 3 details the low-frequency dynamics with the observation of a soft mode. In section 4, the high-frequency dynamics is explored. The character of the transition and the electron–phonon coupling are successively analysed.

2. Experimental details

Single crystals were synthesized and grown by the 'plate-sublimation' method according to Karl [21]. The samples present themselves as plates of approximate dimensions $2 \times 3 \times 1.5$ mm and are very dark.

The infrared spectra were recorded with a Beckman Fourier spectrophotometer (model RS-720). Due to the dimensions of our crystals, we have been forced to use a sample which is a mosaic obtained with different single crystals. The consequence is that the polarization of the modes cannot be known. Another experimental difficulty is that our low-temperature equipment does not permit temperatures lower than 82 K to be acheived. Thus, the low-

temperature phase of TTF-CA is unfortunately inaccessible. We will also underline the fact that, due to the high absorption of the sample, no mode was observed above 40 cm^{-1}.

The Raman spectra were recorded with a DILOR *XY* spectrometer using a CCD detector which is very sensitive in the near-infrared range. Due to the high absorption of TTF-CA in the visible range, the spectra were obtained with a titanium–sapphire laser (Spectra Physics, model 3900 S) at 720.2 nm, which corresponds in the neutral phase to the minimum of the sample absorption curve. Furthermore, the laser beam power was adjusted to around 5–6 mW to reduce sample heating and risks of crystal damage. The low-temperature measurements were carried out inside a Meric cryostat where samples were cooled down by a controlled stream of cold helium gas. The temperature stability is better than 0.1 K.

The infrared experimental lines were refined by the numerical method of Rosenbrock [22]. The Raman modes were deconvoluted from the resolution function and then refined by a least-squares method [23].

3. Low-frequency dynamics: soft-mode observation

The previous Raman and infrared studies have only been concerned with the intramolecular vibrations [11]. In contrast, the lattice modes have not been yet observed.

From the group theory analysis, the classification of the optical lattice modes is as follows in each phase:

$$\Gamma^{N}_{TTF-CA} = 6A_g + 6B_g + 5A_u + 4B_u$$

$$\Gamma^{I}_{TTF-CA} = 10A' + 11A''.$$

Between the two phases, the symmetry change is

$$\begin{array}{ccc} A_g & & A_u \\ & \searrow\nearrow\ A' & & \searrow\nearrow\ A'' \\ B_u & & B_g \end{array}$$

In the neutral phase, the gerade modes are only active in Raman scattering and the ungerade modes only operate in infrared absorption. Besides, the B_u lattice modes can be coupled to the CT (e–lph coupling) [7, 8]. So, this electron–phonon coupling can only be studied by infrared absorption in the neutral phase. In the ionic phase, due to the loss of the symmetry centre, all the lattice modes may be active in Raman scattering and infrared absorption. Thus, the e–lph coupling can be studied by these two techniques in this phase (A' modes).

3.1. Infrared results

In the neutral phase, the 20–35 cm^{-1} spectral range of the infrared spectrum of TTF-CA has been recorded from room temperature to 82 K. Figure 1 shows this spectrum for four representative temperatures. To our knowledge, these spectra are the first experimental representation of TTF-CA low-frequency infrared modes. Between 20 and 35 cm^{-1}, four modes are observed. When the temperature decreases, the modes 1 and 4 present a usual hardening whereas the modes 2 and 3 become softer and softer. Figure 2 presents the evolution versus temperature of the frequency of these four modes. When the temperature decreases, the frequency of mode 3 (30 cm^{-1} at 200 K) decreases at and after 120 K. At the same time, mode 2 (27.5 cm^{-1} at 200 K) is rejected by this decrease. From 95 K to the neutral-to-ionic phase transition temperature (T_{N-I}), the frequency of mode 3 stabilizes at

27.5 cm^{-1}. It can be noted that this frequency corresponds to the frequency of mode 2 at 150 K. On the other hand, near T_{N-I}, the decrease of mode 2 becomes critical and it crosses over mode 1 without consequence. At 82 K, the frequency of the mode 2 is 21 cm^{-1}.

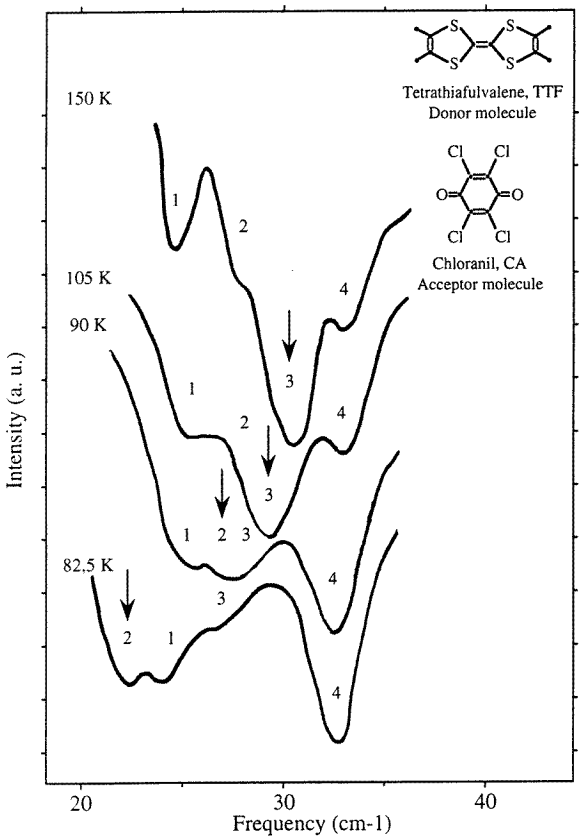

Figure 1. The 20–35 cm^{-1} infrared spectral range of TTF-CA obtained by a mosaic of several single crystals for four representative temperatures in the neutral phase. The arrows represent the soft-mode positions at these temperatures.

The behaviour of modes 2 and 3 is likened to a mode coupling one, and the exchange of character is located near 110 K. Thus, if we take this coupling into account, the decrease of mode 3 is around 9 cm^{-1} between 150 and 82 K in the neutral phase. Besides, this behaviour is like that of a soft mode and the observation of this critical softening, associated with the dimerization, lays emphasis on the displacive nature of the neutral-to-ionic phase transition of TTF-CA at atmospheric pressure. Nevertheless, this important result must be followed by two remarks.

(i) The lowest temperature reached in this experiment is 82 K because our device does not make possible the study below (the ionic phase cannot be studied). Nevertheless, this lowest temperature is near the generally admitted value of T_{N-I} (around 81 K) and the clearly first-order character of the transition demonstrates that the soft-mode frequency is not equal to zero at T_{N-I}. Thus, the lowest frequency which has been observed ($\approx$ 21 cm^{-1}) may not be very different from the soft-mode frequency at T_{N-I}.

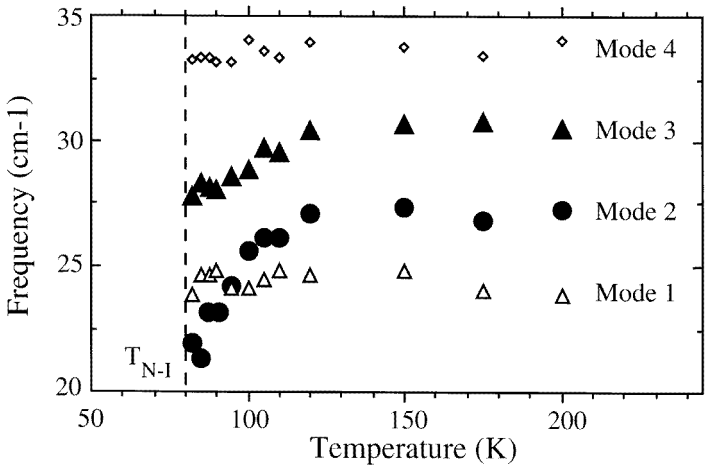

Figure 2. The frequency evolution versus temperature of the u lattice modes of TTF-CA for the 20–35 cm^{-1} spectral range.

(ii) Our spectra are unpolarized because the sample used is a mosaic mode of several single crystals. Thus, the symmetry (B_u) of the mode associated with the dimerization [12] (figure 3) cannot be verified and it would be interesting to confirm the polarization of this mode by an experiment performed with a single crystal of adequate dimensions.

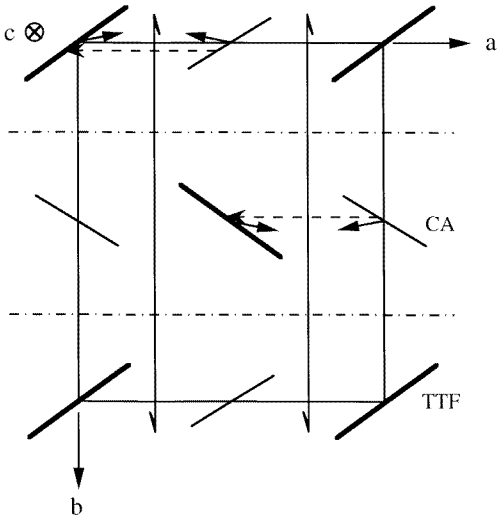

Figure 3. A representation [12] of the B_u mode (full arrows) responsible for the dimerization (dashed arrows) observed in the low-temperature phase. The symmetry elements are shown.

3.2. Raman results

The Raman study of the lattice dynamics has been carried out from 16 to 300 K. Figure 4(a) presents the evolution of the lattice dynamics Raman spectrum at different temperatures

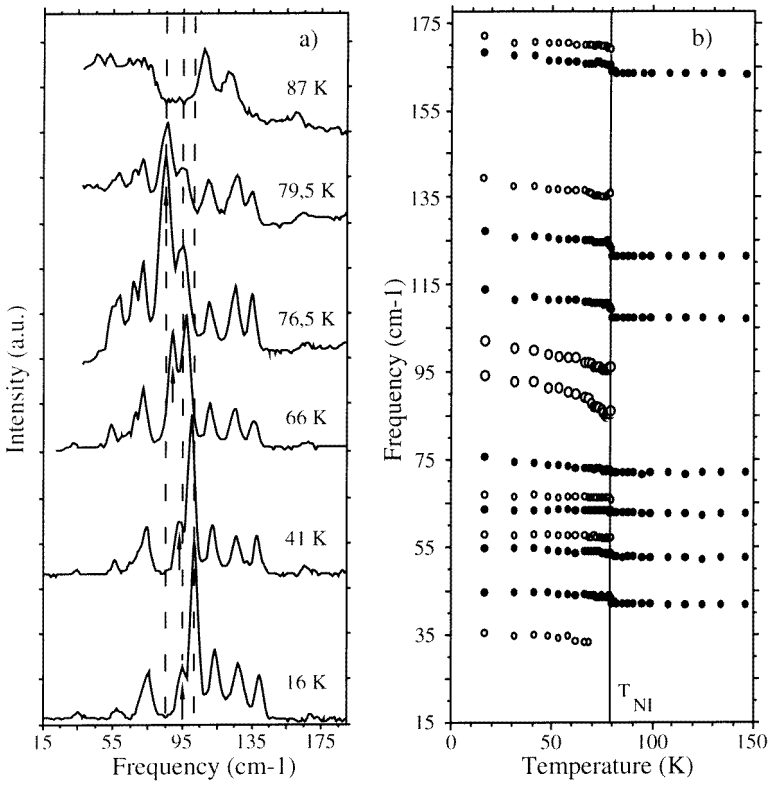

Figure 4. (a) The evolution versus temperature of the 15–190 cm^{-1} Raman spectral range of TTF-CA in the neutral phase (87 K), in the coexistence zone (79.5 K) and in the ionic phase (16, 41, 66 and 76.5 K). In the ionic phase, the arrows show the soft-mode frequencies. (b) The frequency dependence on temperature of the Raman active modes of TTF–CA in the neutral and ionic phases, for the 15–180 cm^{-1} spectral range.

for the neutral and ionic phases. To our knowledge, these low-frequency Raman spectra correspond to the first observation of lattice mode in these systems by Raman spectroscopy. This observation has been possible by using a titanium–sapphire laser coupled to CCD detection. In the 15–185 cm^{-1} spectral range, figure 4(a) shows the high-temperature phase spectrum ($T = 87$ K), four low-temperature phase spectra ($T = 16, 41, 66$ and 76.5 K) and, at $T = 79.5$ K, a spectrum where the modes of both phases are observed simultaneously. Note that, in the low-temperature phase, below 76.5 K, it has been possible to record down to 15 cm^{-1}. On the other hand, due to a large enhancement of the elastic and/or quasi-elastic scattering line, the lower limit of recording is around 40 cm^{-1} in the vicinity of T_{N-I} in the low temperature phase and in the high-temperature phase. Figure 4(b) presents the frequency evolution of the different modes which are observed in the 40–180 cm^{-1} spectral range for the neutral phase, and in the 15–180 cm^{-1} for the ionic phase.

At first, the transition is characterized by an increase in the number of modes. Seven modes are observed in the neutral phase; fourteen are observed in the ionic phase (figure 4(b)). The loss of the symmetry centre explains this observation. The u modes, only active in infrared absorption in the neutral phase, become active in Raman scattering in the ionic phase. In the neutral phase (figure 4(b)), an usual hardening has been observed between

room temperature and T_{N-I}. At the transition, several g modes present a discontinuity of their frequency:

(i) 3.5 cm^{-1} for the modes located at 107 and 121 cm^{-1} at 87 K
(ii) 1.5 cm^{-1} for the modes located at 42 and 163 cm^{-1} at 87 K and
(iii) < 1 cm^{-1} for the modes located at 53, 63 and 72 cm^{-1} at 87 K.

These frequency discontinuities of g modes traduce the first-order character of the neutral-to-ionic phase transition of TTF-CA. These frequency discontinuities and the appearance of u modes which occur simultaneously (figure 4(b)) have been used to define the neutral-to-ionic phase transition temperature T_{N-I} which is so estimated at 78 K for this experiment (figure 4(b)). The difference between this value and the usual T_{N-I} (81 K) could be assigned to a local heating of the sample due to the impact of the laser beam on the crystal.

In the ionic phase, at the approach of T_{N-I}, a critical softening of the mode located at 95 cm^{-1} at 16 K is observed. This soft mode disappears at T_{N-I}. In the 15–180 cm^{-1} spectral range, this mode is the only one which presents such an anomaly. Moreover, studies in polarized light have shown that the symmetry of this mode is A′. Besides, the representation of the mode associated to the dimerization is B_u in the high-temperature phase and A′ in the low-temperature phase. Therefore, the B_u representation is an unidimensional one, so only one soft mode is expected in the low-temperature phase. Thus, this Raman mode seems to correspond to the soft mode observed by infrared absorption in the neutral phase and can be assigned to the dimerization observed in the ionic phase.

In another way, the Raman soft mode seems to be coupled to the mode located at 102 cm^{-1} at 16 K. The frequency of this second mode decreases from 102 cm^{-1} to 95 cm^{-1} between 16 K and T_{N-I}, this latter frequency corresponding to the Raman soft-mode frequency at 16 K. Moreover, between 40 and 70 K, the exchange of intensity (figure 4(a)) is another argument for this coupling. Therefore, in the ionic phase, if we take this coupling into account, the soft mode frequency decreases by 17 cm^{-1}.

The softening observed by Raman scattering in the ionic phase corroborates our result obtained by infrared absorption in the neutral phase. Thus, these infrared and Raman studies show the displacive nature of the neutral-to-ionic phase transition of TTF-CA. However, the ionic frequency of the soft mode is highly superior to that of the neutral one, and such a difference may be surprising, but with the first-order character of this transition and the dimerization (decrease of the (DA) distance), a large hardening of this mode is expected between the neutral and ionic phases. Finally, it can be noted that such a discontinuity has also been observed on the displacive dynamics of *p*-terphenyl-D [23, 24] and of A-TCNB [22, 25].

To conclude this low-frequency dynamics study, we must notice that, in both the neutral and ionic phases, the frequency evolution versus temperature of this soft mode cannot be described by Landau theory. Therefore, this mode can be influenced by the e–lph coupling. Thus, this displacive nature of the neutral-to-ionic phase transition of TTF-CA is not a purely structural one.

4. High-frequency Raman study

As previously seen, the whole spectral range of internal modes has been recorded by Girlando *et al* [11] at room temperature and at 15 K. So, the aim of our study is to analyze the internal mode behaviour through the neutral-to-ionic phase transition of TTF-CA.

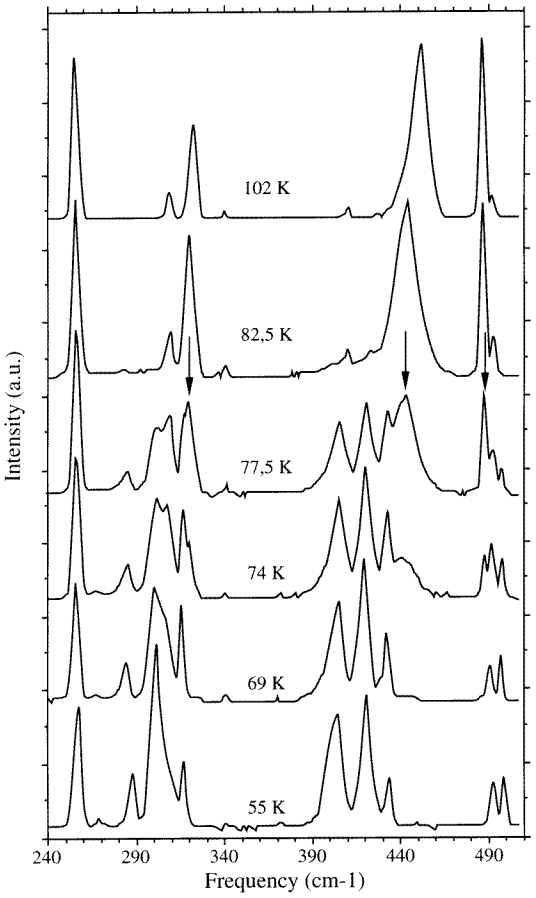

Figure 5. The evolution versus temperature of the 240–510 cm^{-1} Raman spectral range of TTF–CA in the neutral phase (102, 82.5 K), in the coexistence zone (77.5, 74 K) and in the ionic phase (69, 55 K). The arrows indicate the lines which are assigned to *g* modes in the neutral phase and which disappear below T_{N-I}.

4.1. The coexistence zone and transition character

Figure 5 presents the evolution of the Raman spectrum versus temperature for the 240–510 cm^{-1} spectral range. The agreement between these spectra and those of Girlando *et al* [11] is satisfactory. Nevertheless, it should be noted that we observe two additional lines (located at 269 and 286 cm^{-1}) in the ionic phase spectrum (figure 5, $T = 55$ K). The observation of these lines may be due to the fact that our experiment has been performed with an oriented single crystal. In our spectra, nine and sixteen modes have been respectively observed in the neutral and ionic phases for the 240–510 cm^{-1} spectral range. This increase in the number of modes is due to the symmetry breaking. Around the transition, the intensity behaviour of the u modes which appear in the ionic phase is used to define T_{N-I} (figure 6). So, from this experiment T_{N-I} is estimated at 75 K, and the difference (≈ 3 K) between this temperature and the value obtained from the lattice dynamics study (≈ 78 K) is assigned to the important heating of the sample.

On the other hand, nineteen modes are observed in the Raman spectrum around the

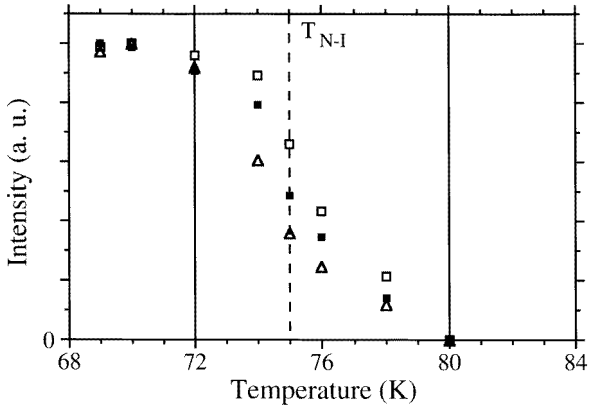

Figure 6. The evolution versus temperature of the u mode intensity of TTF-CA in the coexistence zone. At 55 K (figure 5), these modes are located at 285 (□), 301 (■) and 401 cm^{-1} (△). The temperature domain between vertical lines corresponds to the coexistence zone observed by Raman scattering.

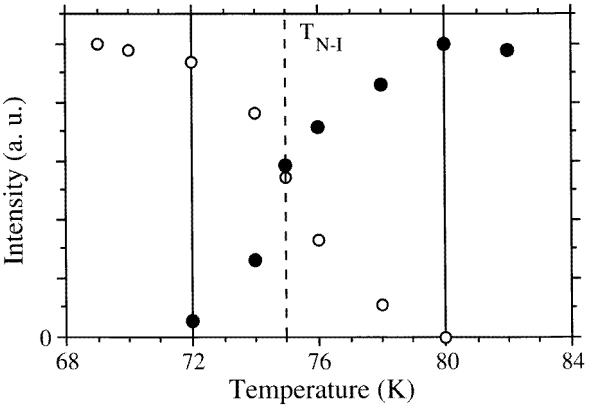

Figure 7. The evolution versus temperature of the intensity of the neutral (●) and ionic (○) lines assigned to the CA-$a_g\nu_4$ mode of TTF-CA. The temperature domain between vertical lines corresponds to the coexistence zone observed by Raman scattering.

transition temperature (figure 5, $T = 77.5$ and 74 K). This anomaly produces a coexistence of the neutral and ionic phases. From the high- to the low-temperature phase, we respectively define the beginning and the end of this coexistence zone by

(i) The appearance in the neutral phase spectrum of modes which are only active in the ionic phase and

(ii) the disappearance of lines which are active in the neutral phase. Figure 5 shows that three lines observed in the neutral phase spectrum disappear at a temperature lower than T_{N-I}. This observation explains the presence of nineteen bands in the coexistence zone and of sixteen bands in the ionic phase.

In the neutral phase near T_{N-I}, these three bands are respectively assigned to the CA-$a_g\nu_4$ (located at 487 cm^{-1}), TTF-$a_g\nu_6$ (located at 443 cm^{-1}) and CA-$a_g\nu_5$ (located at 319 cm^{-1}) modes (Girlando's notation [11]). On the other hand, in the ionic phase

near T_{N-I}, these three modes correspond to the bands located at 498, 433 and 315 cm^{-1} respectively. So, in the coexistence zone, the spectra of both phases are present. This fact explains the apparent anomaly in the number of bands. Note that concerning the assignments of these three modes we have used those of Girlando *et al* in the neutral phase [11]. On the other hand, our study of the TTF-CA phase transition at low temperature under pressure [26], where it becomes more continuous, has permitted the modification of some of Girlando's assignments in the ionic phase.

Figure 7 presents the evolution versus temperature of the intensity of the neutral and ionic lines assigned to the CA-$a_g\nu_4$ mode. This figure shows that the ionic line appears at the same temperature (around 80 K) as the bands assigned to u modes (figure 6), and the neutral line disappears below 72 K. Under these conditions, the coexistence zone can be evaluated on a 8 K temperature range. This value is much greater than the one (from 1.5 to 3 K) observed by neutron diffraction [12] and RQN [27] studies. Note that, for these two experiments, the coexistence zone is attributed to an intrinsic coexistence of the neutral and ionic phases. On the other hand, the origin of the Raman coexistence is essentially assigned to a gradient of temperature associated to the high absorption of the sample and to the inhomogeneous distribution of energy in the laser beam. This extrinsic character explains the great discrepancy between these results. Therefore, Raman scattering is not a good technique for the study of the intrinsic coexistence of the neutral and ionic phases of TTF-CA.

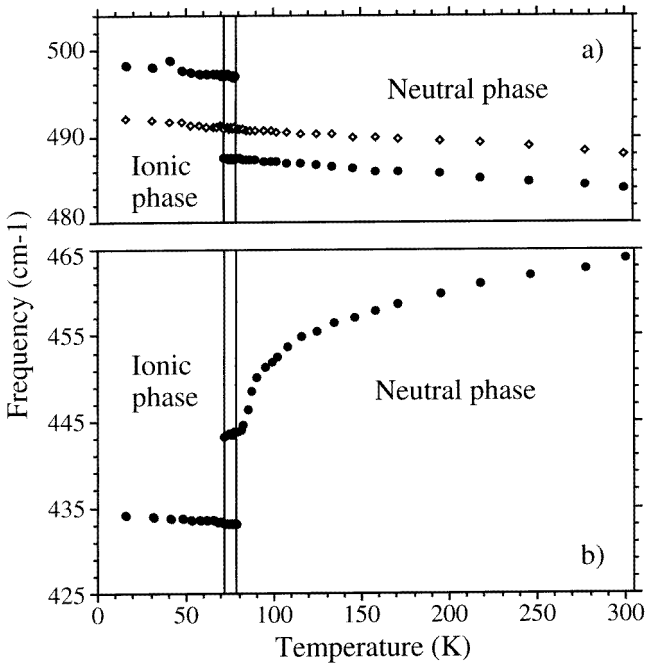

Figure 8. The frequency dependence on temperature of two totally symmetric molecular modes of TTF-CA: (a) ● , CA-$a_g\nu_4$ mode; (b) ● , TTF-$a_g\nu_6$ mode. The temperature domain between vertical lines corresponds to the coexistence zone observed by Raman scattering. (a) shows also the frequency dependence on temperature of another mode belonging to this spectral range.

In the evolution of this 240–510 cm^{-1} spectral range versus temperature, another interesting point is the observation of frequency jumps through the transition for the above-

mentioned three modes. These discontinuities, equal to 10 cm^{-1} for the CA-$a_g\nu_4$ mode (figure 8(a)), 10 cm^{-1} for the TTF-$a_g\nu_6$ mode (figure 8(b)) and 4 cm^{-1} for the CA-$a_g\nu_5$ mode, show unambiguously the first-order character of the TTF-CA phase transition at atmospheric pressure.

4.2. High frequency: e–mv coupling

Totally symmetric molecular a_g modes are quite interesting because, for symmetry reasons, they are the only ones which can couple with electrons [7, 8]. Due to the interaction with the CT excitation within the crystal, the a_g modes frequencies (ω_{pi}) will be lowered with respect to that of the unperturbed D and A molecules (ω_i) with the same ionicity ρ. The frequency of the Raman lines is in fact determined both by the ionicity ρ and by the e–mv interaction. From the model described by Girlando *et al* [18], we have calculated the e–mv coupling constants g_i of several a_g modes. Table 1 gives the ω_0, ω_+ or ω_- frequencies and the ω_{pi} and ω_i frequencies at 300 and 15 K. The ω_i frequencies are obtained by linear extrapolation versus ionicity from frequencies of neutral molecules (ω_0) and of fully ionic molecules (ω_+ or ω_-) [11, 18]. The modes TTF-$a_g\nu_1$, TTF-$a_g\nu_4$ and CA-$a_g\nu_6$ have not been taken into account in the calculation for different reasons.

(i) For the TTF-$a_g\nu_1$ mode, in the literature [11], no corresponding vibronic absorptions have been observed. Moreover, our own study has not permitted the observation of this mode.

(ii) For the TTF-$a_g\nu_4$ mode, which involves C–H bendings of the TTF molecule, it is known [11] to be strongly affected by crystalline environment.

(iii) For the CA-$a_g\nu_6$ mode, the perturbed frequency (ω_{pi}) is greater than the unperturbed one (ω_i). Therefore, this mode is also affected by crystalline environment.

Table 1 clearly shows that, in both phases, the ω_{pi} frequencies of many a_g modes are inferior to the ω_i ones. This is the expected signature of the e–mv coupling. However, it can be noted that for the TTF-$a_g\nu_2$ and TTF-$a_g\nu_7$ modes, this $|\omega_i - \omega_{pi}|$ frequency difference is weak.

Figure 9 presents the results of our e–mv coupling constant (g_i) calculation. For six modes whose frequency dependence on temperature is known, we have calculated the e–mv coupling constants as a function of temperature. For the other modes (TTF-$a_g\nu_5$, TTF-$a_g\nu_3$, CA-$a_g\nu_1$ and CA-$a_g\nu_2$) these constants are given for $T = 300$ K and $T = 15$ K. The results, taking our new assigments into account, are in agreement with those of Girlando *et al*. At first, it is noted that when the values of the calculated coupling constants are important, they correspond to modes which deform [28, 29] the HOMO (TTF molecule) or the LUMO (CA molecule) orbitals. Besides, in both phases, for the TTF-$a_g\nu_2$ and TTF-$a_g\nu_7$ modes, the e–mv coupling constants are weak. This could explain why the ω_{pi} frequencies of these two modes are not very different from the ω_i frequencies.

Between the neutral and ionic phases, the expected behaviour would be to observe the same g_i constant in both phases [8, 11, 18, 30]. Nevertheless, in figure 9, we can note that six of these e–mv coupling constants present important variations between the high- and low-temperature phases. Indeed, five g_i constants associated with a_g modes increase whereas one decreases.

Concerning the five modes whose g_i coupling constants increase, the frequency behaviour of these modes versus temperature is similar: the frequency decreases in the neutral phase with a slope which increases as the transition approaches. Besides, a jump towards the low frequencies is observed at T_{N-I}. An example corresponding to the TTF-

Table 1. Raman frequencies (ω_0, $\omega_\pm$) corresponding to different totally symmetric molecular modes of TTF^0, CA^0, TTF^+ and CA^- molecules [11, 18], and observed Raman frequencies (ω_{pi}) for these modes in a TTF-CA single crystal for two temperatures (15 and 300 K). The (ω_i) frequencies have been obtained by extrapolating the frequencies of neutral and fully ionic molecules on the basis of $\rho = 0.2$ at 300 K and $\rho = 0.7$ at 15 K.

	TTF^0 $\rho = 0$	TTF-CA (300 K) $\rho = 0.2$		TTF-CA (15 K) $\rho = 0.7$		TTF^+ $\rho = 1$
	ω_0 (cm^{-1})	ω_{pi} (cm^{-1})	ω_i (cm^{-1})	ω_{pi} (cm^{-1})	ω_i (cm^{-1})	ω_+ (cm^{-1})
TTF-$a_g\nu_2$	1555	1543	1545	1521	1520	1505
TTF-$a_g\nu_3$	1518	1445	1498.5	1321	1449.5	1420
TTF-$a_g\nu_5$	735	734	739.5	732.5	758	751
TTF-$a_g\nu_6$	472	464	478	434.5	492.5	501
TTF-$a_g\nu_7$	244	253.5	248.5	257	259	265
	CA^0 $\rho = 0$	TTF-CA (300 K) $\rho = 0.2$		TTF-CA (15 K) $\rho = 0.7$		CA^- $\rho = 1$
	ω_0 (cm^{-1})	ω_{pi} (cm^{-1})	ω_i (cm^{-1})	ω_{pi} (cm^{-1})	ω_i (cm^{-1})	ω_- (cm^{-1})
CA-$a_g\nu_1$	1693	1629	1658	1545	1570.5	1518
CA-$a_g\nu_2$	1609	1570	1606	1568	1598.5	1594
CA-$a_g\nu_3$	1007	982	1011.5	943	1022	1028
CA-$a_g\nu_4$	496	484	500.5	498.5	511	517
CA-$a_g\nu_5$	330	325.5	331.5	316.5	335.5	338

$a_g\nu_6$ mode is shown in figure 8(b). Note that for these modes (table 1), except for the TTF-$a_g\nu_3$ one, the ω_i evolution versus ionicity ($\omega_i^{\rho=0.2} < \omega_i^{\rho=0.7}$) is the inverse of the ω_{pi} evolution versus temperature ($\omega_{pi}^{\rho=0.2\ (300\ K)} > \omega_{pi}^{\rho=0.7\ (15\ K)}$). So for these four modes the frequency discontinuity observed at T_{N-I} can be assigned to the increase of the g_i coupling constant. On the other hand, for the fifth mode (TTF-$a_g\nu_3$), table 1 shows that between 300 K ($\rho = 0.2$) and 15 K ($\rho = 0.7$) the expected ω_i change is $\Delta\omega_i = -49\ cm^{-1}$ whereas the observed ω_{pi} change is $\Delta\omega_{pi} = -124\ cm^{-1}$. Here also, the increase of the g_i coupling constant could explain this great discrepancy between $\Delta\omega_i$ and $\Delta\omega_{pi}$.

Concerning the CA-$a_g\nu_4$ mode whose g_i coupling constant decreases between the neutral and ionic phases, the frequency dependence on temperature corresponds essentially to a jump towards the high frequencies through the transition (figure 8(a)). Nevertheless, it must be noted that ω_i increases with the same order of magnitude when ρ rises. Thus, for this mode it is difficult to make conclusions about the influence on the frequency change, of the decrease of the g_i coupling constant through the transition. By another way, it must be noted that for the modes whose coupling constants are weak or do not vary (CA-$a_g\nu_1$) between the neutral and ionic phases, a frequency change in agreement with the ω_i variations as a function of ρ, is also observed.

Thus, for the present, no definitive conclusion can be given on these coupling constant behaviours, but only some comparisons between experimental results and coupling constant calculations can be made.

Finally, it should be noted that in the neutral phase the TTF-$a_g\nu_6$ (figure 10) and CA-$a_g\nu_3$ modes present an important increase of their linewidth in the vicinity of T_{N-I}. These modes, which are highly coupled to the CT, present an important anomaly of their coupling constant at T_{N-I} (figure 9). An interpretation based on order–disorder dynamics cannot be applied to explain this pretransitional linewidth increase, because far from the transition the

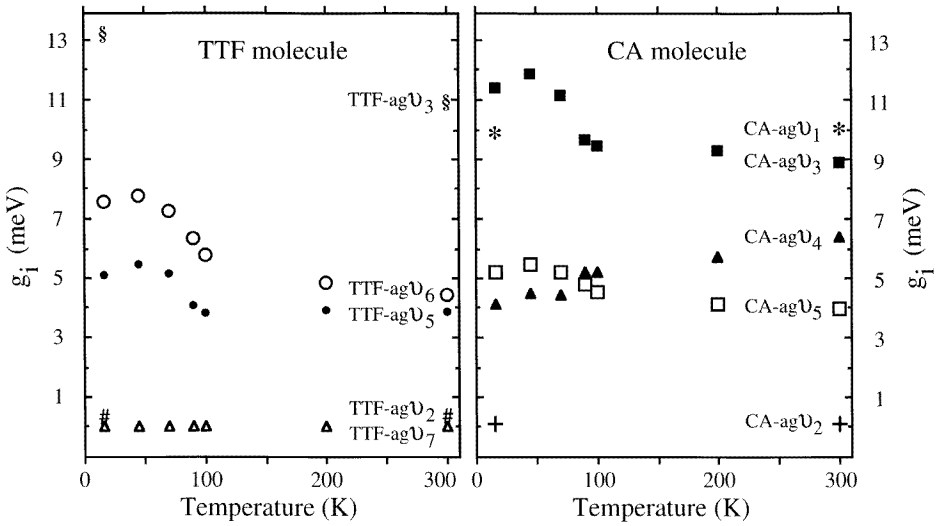

Figure 9. The evolution versus temperature of the e–mv coupling constants (g_i) of different totally symmetric molecular modes of TTF-CA between 300 and 16 K.

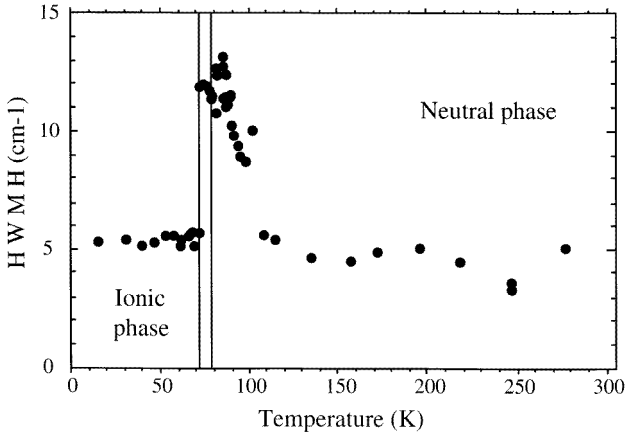

Figure 10. The linewidth dependence on temperature of the TTF-$a_g\nu_6$ totally symmetric molecular mode of TTF-CA. The temperature domain between vertical lines corresponds to the coexistence zone observed by Raman scattering.

neutral and ionic linewidths are similar (note that this agrees with the displacive nature of the transition). So, we must look for another explanation of the origin of this linewidth increase. A hypothesis is to assign this behaviour to the ionicity pretransitional variation in the neutral phase. This ionicity anomaly has been displayed by optical absorption and infrared absorption studies [10] and has been finely analysed by RQN [31]. The RQN result concerning the dependence on temperature of the resonance frequency of the ^{35}Cl shows that the beginning of the frequency decrease is observed between T_{N-I} and $T_{N-I} + 25$ K. This resonance frequency decrease has been assigned to ionicity variations in the vicinity of T_{N-I}. This above-mentioned temperature domain corresponds approximately to that of

the linewidth increase of the TTF-$a_g\nu_6$ (figure 10) and CA-$a_g\nu_3$ modes. Consequently, these linewidth behaviours are another signature of the interaction between ionicity and molecular vibrations.

The Raman study of the influence of temperature and pressure has been successful. The aim of this work, beyond that of the phase diagram definition, is the determination whether the clearly first-order character of the transition subsists under pressure and to provide information about the evolution of the transition mechanism.

Acknowledgments

We wish to thank sincerely Drs N Karl and K H Kraft from the University of Stuttgart (Germany), for growing the crystals.

References

[1] Torrance J B, Vasquez J E, Mayerle J J and Lee V Y 1981 *Phys. Rev. Lett.* **46** 253
[2] Torrance J B, Girlando A, Mayerle J J, Crowley J I, Lee V Y and Batail P 1981 *Phys. Rev. Lett.* **47** 1747
[3] Batail P, La Placa S J, Mayerle J J and Torrance J B 1981 *J. Am. Chem. Soc.* **103** 951
[4] see e.g. Mulliken R S and Person W B 1969 *Molecular Complexes: a Lecture and Reprint Volume* (New York: Wiley)
[5] see e g, Briegleb G 1961 *Electronen-Donator–Acceptor-Komplexe* (Berlin: Springer)
[6] see e.g. Soos Z G 1975 *Annu. Rev. Phys. Chem.* **25** 121
Soos Z G and Klein J 1974 *Molecular Association* ed R Foster (New York: Academic)
[7] Bozio R and Pecile C 1980 in *The Physics and Chemistry of Low Dimensional Solids* ed L Alcacer (Dordrecht: Reidel)
[8] Pecile C, Painelli A and Girlando A 1989 *Mol. Cryst. Liq. Cryst.* **171** 69
[9] Girlando A, Pecile C, Brillante A and Syassen K 1986 *Solid State Commun.* **57** 891
[10] Jacobsen C S and Torrance J B 1983 *J. Chem. Phys.* **78** 112
[11] Girlando A, Marzola F, Pecile C and Torrance J B 1983 *J. Chem. Phys.* **79** 1075
[12] Le Cointe M, Lemée-Cailleau M H, Cailleau H, Toudic B, Toupet L, Heger G, Moussa F, Schweiss P, Kraft K H and Karl N 1995 *Phys. Rev.* B **51** 3374
[13] Mayerle J J, Torrance J B and Crowley J I 1979 *Acta Crystallogr.* B **35** 2988
[14] Gourdji M, Guibé L, Péneau A, Gallier J, Toudic B and Cailleau H 1992 *Z. Naturfor.* a **47** 257; 1991 *Solid State Commun.* **77** 609
[15] Okamoto H, Mitani T, Tokura Y, Koshihara H, Komatsu T, Iwasa Y, Koda T, Saïto G 1991 *Phys. Rev.* B **43** 8224
[16] Ayache C, Le Cointe M, Lemée-Cailleau M H, Cailleau H 1995 private communication
[17] Tokura Y, Okamoto H, Mitani T, Saïto G and T Koda 1986 *Solid State Commun.* **57** 607
[18] Girlando A, Bozio R, Pecile C and Torrance J B 1982 *Phys. Rev.* B **26** 2306
[19] Girlando A, Pecile C and Painelli A 1983 *J. Physique Coll.* C3, Suppl No 6, T 44 1547
[20] Hanfland M, Brillante A, Girlando A and Syassen K 1988 *Phys. Rev.* B **35** 1456
Hanfland M, Brillante A, Girlando A and Syassen K 1988 *Synth. Met.* **27** 549
[21] Karl N 1989 *Proc. Int. Conf. on Materials for Non-linear and Electro-Optics Ser 103* (Bristol: IOP Publishing) 107
[22] Bourges Ph 1989 *Thesis* University of Rennes
[23] Girard A, Delugeard Y and Cailleau H 1987 *J. Physique* **48** 1751
[24] Cailleau H, Girard A, Messager J C, Delugeard Y and Vettier C 1984 *Ferroelectrics* **54** 257
Launois P 1987 *Thesis* University of Paris Sud (Orsay)
Lemée-Cailleau M H 1989 *Thesis* University of Rennes
[25] Bourges Ph, Ecolivet C, Mierzejewski A, Delugeard Y and Girard A 1989 *Proc. 'Phonons '89' (Heidelberg)*
Bourges Ph, Lemée-Cailleau M H, Launois P, Cailleau H, Moussa F, Ecolivet C, Delugeard Y, Girard A and Mierzejewski A 1989 *Proc. 'Disorder in Molecular Solids' (Garchy)*
[26] Moréac A, Girard A, Delugeard Y 1996 *J. Phys.: Condens. Matter* at press
[27] Le Cointe M, Gallier J, Cailleau H, Gourdji M, Péneau A and Guibé L 1995 *Solid State Commun.* **94** 445

[28] Bozio R, Girlando A and Pecile C 1977 *Chem. Phys. Lett.* **52** 503
Berlinsky A J, Hoyano Y and Weiler L 1977 *Chem. Phys. Lett.* **45** 419
[29] Katan C, Blöchl P E, Margl P and Koenig C 1996 *Phys. Rev.* B at press
[30] Luty T and Kuchta B 1988 *Phys. Rev.* B **37** 5748
Luty T 1988 *J. Phys. Soc. Japan* **61** 3636
[31] Gallier J, Toudic B, Delugeard Y, Cailleau H, Gourdji M, Péneau A and Guibé L 1993 *Phys. Rev.* B **47** 11 688